Dynamic heat capacity in spatially restricted systems with phase transition

2009 J. Phys.: Condens. Matter 21 382201

(http://iopscience.iop.org/0953-8984/21/38/382201)

IOP FTC
IOP PUBLISHING JOURNAL OF PHYSICS: CONDENSED MATTER
J. Phys.: Condens. Matter **21** (2009) 382201 (7pp) doi:10.1088/0953-8984/21/38/382201

FAST TRACK COMMUNICATION

Dynamic heat capacity in spatially restricted systems with phase transition

Artjom Vargunin

Institute of Physics, University of Tartu, 4 Tähe Street, 51010 Tartu, Estonia

E-mail: bh@ut.ee

Received 17 July 2009
Published 17 August 2009
Online at stacks.iop.org/JPhysCM/21/382201

Abstract
The frequency-dependent complex heat capacity has been derived for spatially restricted systems with a bulk phase transition. It is demonstrated that internal energy relaxation is determined by the eigenvalues of the Fokker–Planck operator, providing an insight into the symmetry of the reduced free energy. The size driven properties of the energy relaxation rates are discussed and the universal ratio between them has been found.

1. Introduction

The first notion of frequency-dependent complex heat capacity seems to have appeared in literature at the beginning of the 20th century in scientific works concerning the propagation of sound in various media [1]. Anomalous ultrasonic attenuation in polyatomic gases [2] and the critical attenuation of ultrasound near the critical point [3] have been explained in terms of the dynamic heat capacity. The first measurements using specific heat spectroscopy were made on glycerol near the glass transition [4, 5]. It was shown that the frequency-dependent specific heat of supercooled liquids is directly related to a frequency-dependent longitudinal viscosity [6]. Dynamic calorimetry was recently successfully applied to ferroelectric and ferromagnetic systems [7–12].

Several theoretical approaches for the formulation of the dynamic specific heat were suggested, e.g., generalized hydrodynamics [13], the fluctuation-dissipation theorem [14], projection operator formalism [15], the generalized constitutive equation [16], the framework of the free energy landscape [17], or non-equilibrium considerations [18]. Simulations have been able to reproduce various qualitative features [15, 19]. Nowadays, the dynamic heat capacity continues to be explored from both experimental and theoretical perspectives, in anticipation that dynamic calorimetry would provide an insight into the energy landscape dynamics.

Usually one associates the imaginary part of a linear susceptibility with the absorption of energy by the sample from the applied field. However, in the case of the generalized calorimetric susceptibility there is no net exchange of energy between the sample and the surrounding heat bath during a complete cycle of a frequency-domain specific heat experiment. The imaginary part of the frequency-dependent complex heat capacity is always connected to the net entropy produced during the experimental timescale by oscillatory heat exchange between the sample and the heat bath. This creation of entropy is always due to a particular physical irreversible process in the vicinity of thermodynamic equilibrium, for which the relaxation time plays a major role. If heat is supplied in a shorter time interval than this relaxation time constant, the corresponding internal degree of freedom does not contribute entirely to the equilibrium value of the measured heat capacity under the timescale of observation. In this situation, the measured heat capacity becomes a dynamic quantity. During the relaxation of the slow internal degree of freedom a certain amount of heat is lost, consequently, this amount of heat does not participate in the equilibrium part of the measured heat capacity [20, 21].

In the present communication, we study the peculiarities of the dynamic heat capacity associated with the order parameter distributed in the bistable potential. We consider a soft potential, naturally arising in the Landau theory of the bulk second-order phase transitions [22]. Various size effects on the internal energy relaxation and dynamic heat capacity are investigated by means of the Fokker–Planck equation formalism. Hereafter, we assume that temperature is homogeneous in all parts of the system at any time and it has no time to relax towards the thermal bath.

2. Stochastic equation of motion

We start with the one-dimensional equation of overdamped motion for the temporal evolution of the non-equilibrium order parameter x, namely

$$\frac{\mathrm{d}x(t)}{\mathrm{d}t} = -\frac{\partial \tilde{F}(x;T)}{\partial x} + \sqrt{\frac{T}{V}}\zeta(t). \tag{1}$$

Here $\zeta(t)$ is the zero mean Gaussian white noise with the correlation function $\langle\zeta(t)\zeta(t')\rangle = 2\delta(t-t')$, T is temperature, V is the volume of the sample. The temperature-dependent soft potential $\tilde{F}$ is taken in the Landau form [22]

$$\tilde{F}(x;T) = \frac{\alpha}{2}(T - T_{\mathrm{c}}^{\infty})x^2 + \frac{1}{4}x^4, \tag{2}$$

and has the meaning of non-equilibrium free energy density. Here the constant $\alpha > 0$, and T_{c}^{∞} is the temperature of bulk second-order phase transition. The potential $\tilde{F}(x)$ is bistable if $T < T_{\mathrm{c}}^{\infty}$, and monostable if $T > T_{\mathrm{c}}^{\infty}$.

The considered model describes the sample whose dimensions are smaller than the correlation length of the order parameter fluctuations (analogously to zero-dimensional superconductors [23]). In equation (1) the finiteness of the system induces stochastic motion of the order parameter leading to the existence of the internal noise ζ. The latter vanishes in the bulk limit ($V \to \infty$) leaving us with the Landau–Khalatnikov equation which describes the deterministic relaxation of the order parameter to its equilibrium value. The size driven crossover from stochastic behavior to a deterministic one is a substantial feature of this approach.

Note that in the present scheme the inhomogeneity of the order parameter fluctuations is neglected. Another limiting case is the Gaussian approximation [24], which incorporates the spatial variance of fluctuations, but neglects, first of all, interwell motions in the potential (2). Both of these particular cases stem from the general Landau free energy expansion where the second- and the fourth-order terms, as well as the squared gradient of order parameter, are taken into account.

An alternative description of the stochastic order parameter x may be given in terms of the Fokker–Planck equation formalism for probability density $P(x,t)$

$$\frac{\mathrm{d}P(x,t)}{\mathrm{d}t} = L_{\mathrm{FP}}P(x,t), \tag{3}$$

where

$$L_{\mathrm{FP}} = \frac{\partial}{\partial x}\frac{\partial \tilde{F}(x;T)}{\partial x} + \frac{T}{V}\frac{\partial^2}{\partial x^2} \tag{4}$$

is the Fokker–Planck operator with eigenvalues λ_i and eigenfunctions $\psi_i(x)$. The stationary solution of equation (3) is given by $P_{\mathrm{st}}(x) = \psi_0(x) \sim \exp(-\frac{V\tilde{F}(x;T)}{T})$ and $\lambda_0 = 0$.

3. Dynamic heat capacity

The equilibrium properties of the system are determined by the partition function

$$Z(T,V) = \int_{-\infty}^{\infty} \exp\left\{-\frac{V\tilde{F}(x;T)}{T}\right\}\mathrm{d}x. \tag{5}$$

According to the thermodynamic definition of the internal energy $E = F + TS$, where $F = -T\ln Z$ is the equilibrium free energy and $S = -\frac{\partial F}{\partial T}$ is the entropy, one can find that $E = \langle\varepsilon\rangle_{\mathrm{st}}$ with

$$\varepsilon = V(-\tfrac{1}{2}\alpha T_{\mathrm{c}}^{\infty}x^2 + \tfrac{1}{4}x^4) \tag{6}$$

and $\langle\cdots\rangle_{\mathrm{st}} = \int_{-\infty}^{\infty}\cdots P_{\mathrm{st}}(x)\,\mathrm{d}x$. For the static heat capacity C_0 we correspondingly have

$$C_0 = \frac{\partial}{\partial T}E = \frac{1}{T^2}(\langle\varepsilon^2\rangle_{\mathrm{st}} - \langle\varepsilon\rangle_{\mathrm{st}}^2). \tag{7}$$

The expression (7) agrees with the well-known property that heat capacity in the constant volume case is proportional to the mean value of the squared fluctuations of the internal energy [22].

Recently, the fluctuation-dissipation theorem for the frequency-dependent heat capacity was established [14]. According to this result, the frequency-dependent heat capacity may be expressed within the linear response approximation as a linear susceptibility describing the response of the system to arbitrarily small temperature perturbations away from equilibrium

$$C(\Omega) = \frac{1}{T^2}\left(\langle\varepsilon^2\rangle_{\mathrm{st}} - \mathrm{i}\Omega\int_0^{\infty}\langle\varepsilon(0)\varepsilon(t)\rangle_{\mathrm{st}}\mathrm{e}^{-\mathrm{i}\Omega t}\,\mathrm{d}t\right). \tag{8}$$

Here Ω is the frequency of the temperature 'field' varying in time. Thus, the dynamic heat capacity is a complex number whose real and imaginary parts must obey the Kramers–Kronig relation as a result of causality and linearity.

To obtain the frequency-dependent heat capacity for ε given by equation (6) we have to find the appropriate correlations of x^n with $n = 2, 4$. In accordance with [25], the time correlation $K_{n,m}(t)$ of two random variables, x^n and x^m, can be written in the steady state as

$$K_{n,m}(t) \equiv \langle x(t)^n x(0)^m\rangle_{\mathrm{st}} = \sum_{i\geqslant 0} u_{i,n}v_{i,m}\mathrm{e}^{-\lambda_i t}, \tag{9}$$

with

$$u_{i,n} = \int_{-\infty}^{\infty} x^n\psi_i(x)\,\mathrm{d}x, \tag{10}$$

$$v_{i,m} = \int_{-\infty}^{\infty} x^m\varphi_i(x)P_{\mathrm{st}}(x)\,\mathrm{d}x. \tag{11}$$

Here φ_i are the eigenfunctions of the adjoint Fokker–Planck operator $L_{\mathrm{FP}}^{\dagger}$ and $\varphi_0(x) = 1$. Thus, $u_{0,n} = v_{0,n} = \langle x^n\rangle_{\mathrm{st}}$. For a symmetric (even) potential (2) the stationary probability density $P_{\mathrm{st}}(x) = \psi_0(x)$ is an even function of x and the parity of $\psi_i(x)$ alternates. This gives us $u_{2i+1,2n} = 0$. Truncating the series (9) after the fourth term, we then have

$$K_{2n,2m}(t) = \langle x^{2n}\rangle_{\mathrm{st}}\langle x^{2m}\rangle_{\mathrm{st}} + g_{n,m}\mathrm{e}^{-\lambda_2 t} + h_{n,m}\mathrm{e}^{-\lambda_4 t}, \tag{12}$$

where $g_{n,m} = u_{2,2n}v_{2,2m}$ and $h_{n,m} = u_{4,2n}v_{4,2m}$. Note that the expansion (9) stops after a certain term, strictly speaking, only

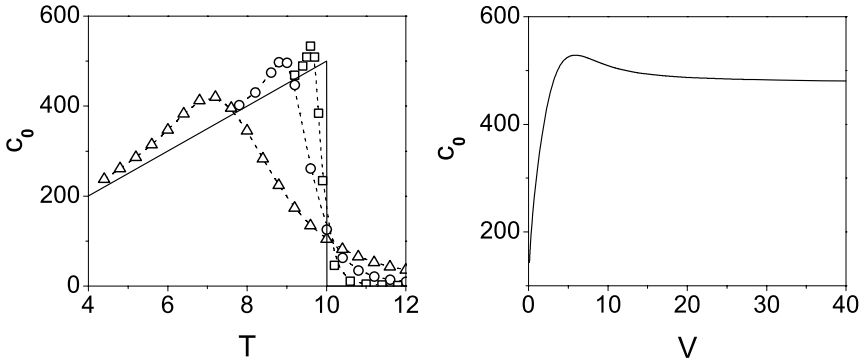

Figure 1. The plots of the static specific heat capacity c_0 versus temperature T (left) for various volumes $V = 0.1$ (triangles), $V = 1$ (circles), $V = 10$ (squares), $V \to \infty$ (solid curve) and versus volume V (right) for fixed temperature $T = 9.5$. Here we use $T_c^\infty = 10$ and $\alpha = 10$.

for a harmonic potential. According to the standard definition of $K_{n,m}(t)$ one can obtain

$$K_{2n,2m}(0) = \int_{-\infty}^{\infty} x^{2n+2m} P_{\rm st}(x)\,{\rm d}x = \langle x^{2n+2m}\rangle_{\rm st}, \tag{13}$$

$$\dot{K}_{2n,2m}(0) = \int_{-\infty}^{\infty} (L_{\rm FP}^{\dagger} x^{2n}) x^{2m} P_{\rm st}(x)\,{\rm d}x$$
$$= -2n\left\langle \frac{\partial \tilde{F}(x;T)}{\partial x} x^{2n+2m-1}\right\rangle_{\rm st} + \frac{T}{V} 2n(2n-1)$$
$$\times \langle x^{2n+2m-2}\rangle_{\rm st}, \tag{14}$$

where the dot denotes the derivative with respect to t. The comparison of equations (13) and (14) with (12) gives

$$g_{n,m} = \langle x^{2n+2m}\rangle_{\rm st} - \langle x^{2n}\rangle_{\rm st}\langle x^{2m}\rangle_{\rm st} - h_{n,m}, \tag{15}$$

$$h_{n,m} = \frac{\dot{K}_{2n,2m}(0) + \lambda_2(\langle x^{2n+2m}\rangle_{\rm st} - \langle x^{2n}\rangle_{\rm st}\langle x^{2m}\rangle_{\rm st})}{\lambda_2 - \lambda_4}. \tag{16}$$

Using above equations, we obtain the frequency-dependent heat capacity by means of the fluctuation-dissipation theorem (8), namely

$$C(\Omega) = C_0\left(\frac{a}{a+b}\frac{\lambda_2}{\lambda_2 + {\rm i}\Omega} + \frac{b}{a+b}\frac{\lambda_4}{\lambda_4 + {\rm i}\Omega}\right), \tag{17}$$

where

$$a = \alpha^2 T_c^{\infty 2}\frac{g_{1,1}}{4} - \alpha T_c^{\infty}\frac{g_{1,2}+g_{2,1}}{8} + \frac{g_{2,2}}{16}, \tag{18}$$

$$b = \alpha^2 T_c^{\infty 2}\frac{h_{1,1}}{4} - \alpha T_c^{\infty}\frac{h_{1,2}+h_{2,1}}{8} + \frac{h_{2,2}}{16}. \tag{19}$$

The static heat capacity (7) may be written in terms of a and b as $C_0 = \frac{V^2}{T^2}(a+b)$.

The frequency-dependent heat capacity (17) indicates that generally for the symmetric (even) potential the timescales of the energy relaxation are defined by the even eigenvalues of the Fokker–Planck operator. For the harmonic potential only the second eigenvalue of the appropriate Fokker–Planck operator contributes to the relaxation process [14]. For the asymmetric (odd) potential non-zero time correlations $K_{2n+1,m}(t)$ appear. This implies that the odd part of the spectrum $\{\lambda_i\}$ will be also involved in the energy relaxation. Thus, the frequency-dependent heat capacity provides an insight into the symmetry of the reduced free energy $\tilde{F}$ and internal energy ε. In contrast to the prediction our model makes on the energy relaxation, it is rather the dominance of the lowest odd eigenvalues (e.g., λ_1, λ_3) that has been obtained for the order parameter relaxation [26].

While the order of glass transition is still under discussions (see, for instance, [4, 27–29]), very similar suggestions were recently made for glassy dynamics described by the two-level model [30, 31]. Namely, if one visualizes the β-processes originating from activated dynamics within a metabasin, where escape from one metabasin to another is taken to describe an α-process within the landscape paradigm of glassy dynamics, then for a symmetric double well only the β-peak appears in the frequency spectrum of the imaginary part of the dynamic heat capacity. However, it is rather the predominance of the α-peak that has been observed for the dielectric relaxation.

4. Results and discussion

Let us analyze the volume-dependent peculiarities of the internal energy relaxation and the dynamic heat capacity. In figure 1 the static specific heat capacity $c_0 = C_0/V$ is illustrated. In the temperature scale this quantity has a volume-dependent maximum. As the volume increases, c_0 approaches its bulk limit, known from the conventional Landau phase transition theory, namely $\alpha^2 T/2$ for $T < T_c^\infty$ and 0 for $T > T_c^\infty$. To obtain the bulk values analytically, one has to compute the weak noise limit, evaluating the moments $\langle x^n\rangle$ by means of parabolic cylinder functions [32].

As the temperature is fixed, one can get enhancement of the static specific heat capacity compared with its bulk value by changing the volume of the system. For temperatures below T_c^∞ the maximum of c_0 appears for a finite sample. As the temperature increases the maximum of c_0 shifts to larger volumes, approaching the bulk value for $T = T_c^\infty$. This behavior can be related to the existence of the critical size [33].

The latter deviations from the Landau-like behavior are essentially stochastic effects. One can relate the critical region (more precisely, the pseudocritical one [34]) with the temperature region where the static specific heat capacity approaches its maximal value. While the internal energy itself increases with temperature in the ordered phase, the dispersion

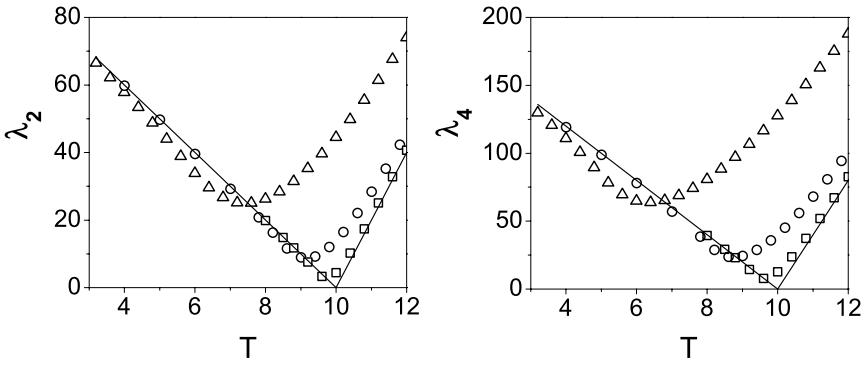

Figure 2. The plots of the eigenvalues λ_2 and λ_4 versus temperature for various volumes $V = 0.1$ (triangles), $V = 1$ (circles), $V = 10$ (squares) and bulk limit $V \to \infty$ (solid curve). Here we use $T_c^\infty = 10$ and $\alpha = 10$.

(fluctuations) of the internal energy approaches the maximal value at the corresponding critical temperature. The decrease of the volume leads to a noise driven redistribution of the probability density (between essentially bi- and monostable structure) at slightly lower temperatures. As the result, one observes a lowering of the critical temperature with volume decrease. The phase transition becomes diffuse due to the fluctuational corrections to the Landau-type behavior. Similar effects were also revealed experimentally in ferroelectrics. Here the temperature of the specific heat jump appears to be dependent on the film thickness or particle size, and there was a distribution of these temperatures: the width became larger with a temperature decrease [35–37]. This size driven behavior is typical for the spatially restricted systems under consideration [26]. An appropriate analysis of the static specific heat in small superconducting particles was also made for the complex order parameter in [23].

The eigenvalues $\lambda_{2,4}$ were calculated numerically, solving the corresponding Schödinger-like equation [38] by means of the symplectic method, see, e.g., [39]. The energy relaxation rates $\lambda_{2,4}$ behave non-monotonically in the temperature scale (see figure 2), having a minimum in the bistable region. A similar behavior of the relaxation rates for the heat capacity was also established experimentally near the ferroelectric phase transition point [10]. As the volume increases, the minimum of $\lambda_{2,4}$ shifts towards the bulk critical temperature T_c^∞. This is a consequence of the volume-dependent noise: in larger samples the dynamics of the relaxation becomes critical at higher temperatures. Moreover, the minimum of $\lambda_{2,4}$ becomes deeper with a volume increase and $\min \lambda_{2,4} \to 0$ as $V \to \infty$. A very similar non-monotonicity of $\lambda_{2,4}$ also appears in the volume scale when the temperature is kept fixed: for $T < T_c^\infty$ the eigenvalues have a minimum for a finite sample which shifts to larger volumes and becomes deeper as $T \to T_c^\infty$.

In the bulk limit for $T < T_c^\infty$ we get

$$\lambda_2 \to \alpha(T_c^\infty - T), \qquad \lambda_4 \to 2\alpha(T_c^\infty - T), \tag{20}$$

and for $T > T_c^\infty$

$$\lambda_2 \to 2\alpha(T - T_c^\infty), \qquad \lambda_4 \to 4\alpha(T - T_c^\infty). \tag{21}$$

Notably that the linearization of the free energy (2) above T_c^∞ leads to the harmonic (therefore, symmetric) potential with the second and the fourth eigenvalue given in equation (21). For the harmonic potential only the second eigenvalue contributes to the dynamic heat capacity, i.e., above T_c^∞ in the bulk limit $a \neq 0$ and $b = 0$ in equation (17). However, the linearization below T_c^∞ leads to the shifted harmonic (asymmetric) potential with the first eigenvalue $2\alpha(T_c^\infty - T)$. Due to asymmetry, the latter governs the leading time dependence in the time correlation of the internal energy. Thus, below T_c^∞ in the bulk limit $a = 0$ and $b \neq 0$ in equation (17). The computation of the weak noise limit leads to the same results. Therefore, for the bulk dynamic heat capacity the leading timescale is given by $2\alpha|T_c^\infty - T|$ above and below T_c^∞. On the other hand, in case of bulk susceptibility the corresponding timescales are different above and below T_c^∞, namely, $2\alpha(T_c^\infty - T)$ for $T < T_c^\infty$ and $\alpha(T - T_c^\infty)$ for $T > T_c^\infty$ [40]. Consequently, the 'law of two' [22] is valid for the order parameter relaxation, but is violated for the energy relaxation.

As the volume increases the heat capacity will contain a contribution which relaxes increasingly slowly near the transition temperature, leading to a longer waiting time for the energy to attain its equilibrium value ($\Omega > \lambda_{2,4}$). Therefore, in real measurements the energy response will show a time delay, and one can expect that the dynamic heat capacity will contain the information about this slow dynamics. On the other hand, when the dynamics of the system occurs at a rate faster than the probing frequencies $\Omega < \lambda_{2,4}$, then the energy relaxes faster to its equilibrium value and the dynamic heat capacity will coincide with its usual static value. In this case the modulus of the heat capacity is determined mostly by the real part, and its imaginary part is small. Unlike the bulk limit, in the finite sample the dynamic heat capacity becomes frequency independent at low frequencies $\Omega < \lambda_{2,4}$ due to $\min \lambda_{2,4} \neq 0$ (figure 3). In particular, it means that in finite sample the energy relaxes faster than the order parameter. As the frequency increases ($\Omega > \min \lambda_2$), the critical region of the finite sample contributes to the dynamic capacity. As a result, its imaginary part rapidly increases, while its real part tends to decrease. The peak of the modulus gets smaller in height and more rounded (see also [7, 41]). For frequencies $\min \lambda_2 < \Omega < \min \lambda_4$

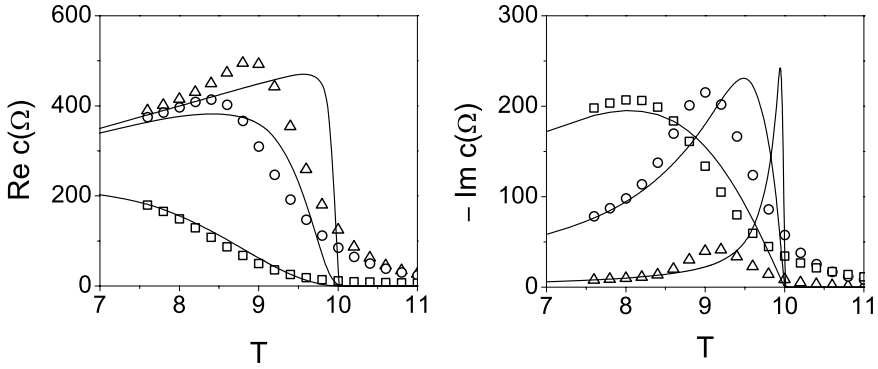

Figure 3. The plots of the real and imaginary part of the dynamic specific heat capacity c versus temperature for $V = 1$ (points) and $V \to \infty$ (solid curves) with frequencies $\Omega = 1$ (triangles), $\Omega = 10$ (circles) and $\Omega = 50$ (squares). For the bulk limit the frequency increases from the right curve to the left one. Here we use $T_c^{\infty} = 10$ and $\alpha = 10$.

overlapping between real and imaginary parts occurs. A further increase in frequencies ($\Omega > \min \lambda_4$) leads to the monotonic decrease of both parts. The dynamic heat capacity for the restricted system becomes almost indistinguishable from its bulk value at high frequencies. One can conclude that there is a crossover between the stochastic and deterministic behavior of the energy response, which is supported by the finite minimal value of the energy relaxation rate in finite samples. Similar complementarity between the stochastic and deterministic response of the order parameter was recently established in terms of the dynamic susceptibility [42]. These peculiarities are closely related to the stochastic nature of the order parameter in the finite sample experiencing, in the bulk limit, deterministic behavior and the second-order phase transition.

According to the formalism of De Donder–Prigogine–Defay, the dynamic heat capacity obtained is the consequence of irreversible thermodynamics near equilibrium in the linear regime [20]. The thermodynamic irreversibility of a peculiar degree of freedom inside the sample is the explanation of the frequency-dependent heat capacity. The time-averaged irreversibility power and time-averaged irreversible entropy production is directly proportional to the imaginary part of the complex heat capacity. Thus, as the frequency of the temperature perturbation or volume of the system increases the thermodynamic irreversibility of the critical region increases. Therefore, the complementarity between stochastic behavior in small systems and deterministic behavior in large systems is accompanied by a crossover between the reversible and irreversible thermodynamics of the critical region.

The phenomenological finite-size scaling theory states, that when the correlation length $\xi(T)$ in the vicinity of the critical temperature attains a magnitude of the order of the characteristic size L of a finite system, deviations from the genuine critical behavior will set in: the singularities in the thermodynamic functions become rounded extrema located in somewhat shifted positions [34, 43, 44]. It is predicted that the finite-size effects on the critical phenomenon are controlled by the ratio L/ξ. This assertion determines the shift of the critical temperature of a finite-size system, particularly, the lowering of T_c as the dimension decreases

$$T_c = T_c^{\infty} - AL^{-\frac{1}{\nu}}, \tag{22}$$

where A is a non-universal positive constant and ν is the critical exponent of the correlation length ξ. From figures 1 and 2 it follows that in the critical region the heat capacity and the energy relaxation times $\lambda_{2,4}^{-1}$ have a maximal value. For further analysis, we will be interested in the temperatures at which the relaxation time λ_2^{-1} takes its maximal value, reflecting in such a way a slowdown effect for the energy fluctuations in the given dimension of the sample $L \sim V^{\frac{1}{3}}$. We will associate these temperatures with finite sample (pseudo) critical temperatures T_c. From figure 4 it follows, that the temperature T_c decreases with a decrease of the volume, resembling experimental data [45–47] and our previous results concerning the order parameter relaxation [40]. For sufficiently large systems we obtain $\nu = 0.719$ (for $\alpha = 1$) and $\nu = 0.665$ (for $\alpha = 10$), which is close to the prediction of the hyperscaling relation $\nu \approx \frac{2}{3}$ in the three-dimensional case [22]. In fact, in the Gaussian approximation one has $\nu = \frac{1}{2}$. Thus, in the present approach one can construct the quantity being an analog of the correlation length ξ. This length scale determines the behavior of the critical temperature T_c in sufficiently large samples. However, the appearance of another length scale in sufficiently small systems breaks down the shift equation (22). Namely, the critical temperature behaves in sufficiently small systems as $T_c \sim L^p$, where $p \approx 3$. The approximate relation for the transition temperature was derived in [40]

$$L \sim \rho(T_c)\xi(T_c), \tag{23}$$

where $\xi(T) \sim (T_c^{\infty} - T)^{-2/3}$ has the meaning of the correlation length in the ordered phase and $\rho(T) \sim T^{1/3}$. From equation (23) it follows, that the phase transition in sufficiently large samples ($T_c \approx T_c^{\infty}$) is determined by the condition $L \sim \rho(T_c^{\infty})\xi(T_c) \sim \xi(T_c)$. However, in smaller systems ($T_c \approx 0$) the critical behavior is driven by the thermal fluctuations and $L \sim \rho(T_c)\xi(0) \sim \rho(T_c)$, where the coefficient of proportionality depends on α. This essentially reflects the competition between two characteristic length scales on the critical behavior in the spatially restricted system (see

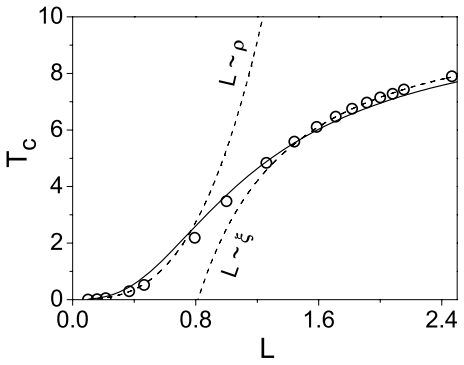

Figure 4. The plot of the critical temperature T_c versus the linear dimension of the system $L = V^{1/3}$ for $\alpha = 1$ (points). The bulk transition temperature is $T_c^{\infty} = 10$. The left dashed line is determined by the condition $L \sim \rho(T_c)$, the right dashed line by the condition $L \sim \xi(T_c)$, i.e. by equation (22). The solid line corresponds to equation (23).

figure 4). The crucial role of the correlation length ξ in large systems has to be devolved to the length ρ in small samples. The length ρ also determines the leading length scale for the transitional behavior in the vicinity of the critical size (see, for details, [40]).

For the energy relaxation rates $\lambda_{2,4}$ we predict, for finite samples, the universal volume-independent ratio at the bulk critical temperature T_c^{∞}, namely

$$R_C = \frac{\lambda_4}{\lambda_2} \simeq 2.86. \qquad (24)$$

For sufficiently low and high temperatures this ratio coincides with the bulk value $R_C = 2$. The value (24) is about two times smaller as compared to $R_\chi = \frac{\lambda_3}{\lambda_1} \simeq 6.04$, found for the rates $\lambda_{1,3}$ of the order parameter relaxation in finite samples [42]. In fact, for glass formers close values of R_χ were derived for both α- and β-relaxation [48].

5. Conclusion

We have obtained and analyzed the dynamic heat capacity by means of the Fokker–Planck equation approach, considering the non-equilibrium order parameter as an internal degree of freedom. The frequency-dependent heat capacity provides an insight into the symmetry of the reduced free energy and internal energy. We have found that in the symmetric case the dynamics of the energy relaxation is determined by the lowest even eigenvalues of the Fokker–Planck operator $\lambda_{2,4}$. In fact, for the order parameter relaxation corresponding rates are given by the lowest odd eigenvalues $\lambda_{1,3}$. The analysis of $\lambda_{2,4}$ shows that the energy relaxation slows down in the critical region. It is demonstrated that the complementarity between stochastic behavior in small systems and deterministic behavior in large systems is accompanied by a crossover between reversible and irreversible thermodynamics of the critical region. The peculiarities of the energy relaxation indicate the size driven competition of the two characteristic length scales in the critical behavior. The crucial role of the correlation length in large systems has to be devolved to the 'fluctuational' length in small samples and, particularly, in the vicinity of critical size. At the bulk transition temperature a universal ratio for the energy relaxation rates $\lambda_{2,4}$ is predicted. Application to the calorimetric measurements in various systems, e.g. ferroelectric particles and ceramics, seems to be possible.

Acknowledgments

The author thank Teet Örd and Risto Tammelo for reading the manuscript and providing helpful suggestions and discussions. This research was supported by the Estonian Science Foundation, Grant No 6789.

References

[1] Alig I 1997 *Thermochim. Acta* **304/305** 35
[2] Herzfeld K F and Rice F O 1928 *Phys. Rev.* **31** 691
[3] Fixman M 1962 *J. Chem. Phys.* **36** 1961
[4] Birge N O and Nagel S R 1985 *Phys. Rev. Lett.* **54** 2674
[5] Birge N O 1986 *Phys. Rev.* B **34** 1631
[6] Zwanzig R 1988 *J. Chem. Phys.* **88** 5831
[7] Jung D H, Kwon T W, Bae D J, Moon I K and Jeong Y H 1992 *Meas. Sci. Technol.* **3** 475
[8] Lee S M and Kwun S I 1994 *Rev. Sci. Instrum.* **65** 966
[9] Moon I K, Jeong Y H and Kwun S I 1996 *Rev. Sci. Instrum.* **67** 29
[10] Bohn K P, Prahm A, Petersson J and Krüger J K 1997 *Thermochim. Acta* **304/305** 283
[11] Shawe J E K, Hütter T, Heitz C, Alig I and Lellinger D 2006 *Thermochim. Acta* **446** 147
[12] Hushur A, Shabbir G, Ko J H and Kojima S 2004 *J. Phys. D: Appl. Phys.* **37** 1127
[13] Jäckle J 1990 *Physica* A **162** 377
[14] Nielsen J K and Dyre C 1996 *Phys. Rev.* B **54** 15754
[15] Scheidler P, Kob W, Latz A, Horbach J and Binder K 1990 *Phys. Rev.* B **63** 104204
[16] Götze W and Latz A 1989 *J. Phys.: Condens. Matter* **1** 4169
[17] Tagawa F and Odagaki T 2008 *J. Phys.: Condens. Matter* **20** 035105
[18] Garden J L 2007 *Thermochim. Acta* **460** 85
[19] Yu C C and Carruzzo H M 2004 *Phys. Rev.* E **69** 051201
[20] Garden J L 2007 *Thermochim. Acta* **452** 85
[21] Garden J L and Richard J 2007 *Thermochim. Acta* **461** 57
[22] Landau L D and Lifshits E M 2000 *Statistical Physics. Part I* (London: Butterworth–Heinemann)
[23] Mühlschlegel B, Scalapino D J and Denton R 1972 *Phys. Rev.* B **6** 1767
[24] Strukov B A and Levanyuk A P 1998 *Ferroelectric Phenomena in Crystals* (Berlin: Springer)
[25] Hänggi P and Thomas H 1982 *Phys. Rep.* **88** 207
[26] Vargunin A, Örd T and Tammelo R 2008 *Phys. Rev.* E **77** 061137
[27] Gutzow I and Petroff B 2004 *J. Non-Cryst. Solids* **345/346** 528
[28] Dimitrov V I 2005 *J. Non-Cryst. Solids* **351** 2394
[29] Wu J 1999 *J. Appl. Polym. Sci.* **71** 143
[30] Chakrabarti D and Bagchi B 2005 *J. Chem. Phys.* **122** 014501
[31] Bisquert J 2005 *Am. J. Phys.* **73** 735
[32] Abramowitz M and Stegun I 1970 *Handbook of Mathematical Functions* (New York: Dover) sections 19.3.7, 19.4.2, 19.8.1 and 19.8.2
[33] Fridkin V M 2006 *Phys.—Usp.* **49** 193
[34] Brankov J G, Danchev D M and Tonchev N S 2000 *Theory of Critical Phenomena in Finite-Size Systems* (Singapore: World Scientific)

[35] Davitadze S T, Kravchun S N, Strukov B A, Goltzman B M, Lemanov V V and Shulman S G 2002 *Appl. Phys. Lett.* **80** 1631
[36] Strukov B A, Davitadze S T, Kravchun S N, Taraskin S A, Goltzman B M, Lemanov V V and Shulman S G 2003 *J. Phys.: Condens. Matter* **15** 4331
[37] Glinchuk M D and Bykov P I 2004 *J. Phys.: Condens. Matter* **16** 6779
[38] Risken H 1996 *The Fokker–Planck Equation* (Berlin: Springer)
[39] Liu X S, Chi Y H and Dong P Z 2004 *Chin. Phys. Lett.* **21** 1681
[40] Vargunin A, Örd T, Tammelo R and Voropajeva N 2008 *J. Phys.: Condens. Matter* **20** 362202
[41] Kuo Y K, Skove M J, Verebelyi D T, Li H, Mackay R, Hwu S J, Whangbo M H and Brill J W 1998 *Phys. Rev.* B **57** 3315
[42] Vargunin A, Örd T and Tammelo R 2008 *Phys. Lett.* A **372** 7187
[43] Fisher M E 1971 *Critical Phenomena* (London: Academic)
[44] Privman V 1990 *Finite Size Scaling and Numerical Simulation of Statistical Systems* (Singapore: World Scientific)
[45] Jiang Q, Cui X F and Zhao M 2004 *Appl. Phys.* A **78** 703
[46] Yang C C and Jiang Q 2005 *Acta Mater.* **53** 3305
[47] Lang X Y and Jiang Q 2007 *J. Nanopart. Res.* **9** 595
[48] Ngai K L 1998 *J. Chem. Phys.* **109** 6982